

The Millennium Galaxy Catalogue: The $M_{\text{bh}}-L_{\text{spheroid}}$ derived supermassive black hole mass function

Marina Vika,^{1,2} Simon P. Driver,^{1,2} Alister W. Graham³ and Jochen Liske⁴

¹*Scottish Universities Physics Alliance (SUPA)*

²*School of Physics & Astronomy, University of St Andrews, North Haugh, St Andrews, Fife, KY16 9SS*

³*Centre for Astrophysics and Supercomputing, Swinburne University of Technology, Hawthorn, Victoria 3122, Australia*

⁴*European Southern Observatory, Karl-Schwarzschild-Str. 2, 85748 Garching, Germany*

Received XXXX; Accepted XXXX

ABSTRACT

Supermassive black hole mass estimates are derived for 1743 galaxies from the Millennium Galaxy Catalogue using the recently revised empirical relation between supermassive black hole mass and the luminosity of the host spheroid. The MGC spheroid luminosities are based on $R^{1/n}$ -bulge plus exponential-disc decompositions. The majority of black hole masses reside between $10^6 M_{\odot}$ and an upper limit of $2 \times 10^9 M_{\odot}$. Using previously determined space density weights, we derive the SMBH mass function which we fit with a Schechter-like function. Integrating the black hole mass function over $10^6 < M_{\text{bh}}/M_{\odot} < 10^{10}$ gives a supermassive black hole mass density of $(3.8 \pm 0.6) \times 10^5 h_{70}^3 M_{\odot} \text{Mpc}^{-3}$ for early-type galaxies and $(0.96 \pm 0.2) \times 10^5 h_{70}^3 M_{\odot} \text{Mpc}^{-3}$ for late-type galaxies. The errors are estimated from Monte Carlo simulations which include the uncertainties in the $M_{\text{bh}}-L$ relation, the luminosity of the host spheroid and the intrinsic scatter of the $M_{\text{bh}}-L$ relation. Assuming supermassive black holes form via baryonic accretion we find that $(0.008 \pm 0.002) h_{70}^3$ per cent of the Universe’s baryons are currently locked up in supermassive black holes. This result is consistent with our previous estimate based on the $M_{\text{bh}}-n$ (Sérsic index) relation.

Key words: galaxies: bulges — galaxies: fundamental parameters — galaxies: luminosity function, mass function — galaxies: nuclei — galaxies: structure — surveys

1 INTRODUCTION

Observations of nearby galaxies have shown that supermassive black holes (SMBHs) exist within the centres of both elliptical galaxies and the classical bulges of disc galaxies (Kormendy & Richstone 1995; Magorrian et al. 1998). At present there are about 50 credible measurements and 26 partial measurements as summarised in Graham (2008b). For lower mass systems ($< 10^8 M_{\odot}$), galaxy cores are dominated by a luminous compact massive object (Graham & Guzmán 2003; Ferrarese et al. 2006; Balcells et al. 2007). Gallo et al. (2008) found AGN activity in early-type galaxies with $M_{\text{gal}} < 10^{10} M_{\odot}$, revealing that SMBHs can exist in low mass galaxies. Furthermore, Satyapal et al. (2008) found SMBHs can form and evolve in bulgeless galaxies. These argue that SMBHs have built up from less massive ‘seeds’ (e.g., Woo et al. 2008). The SMBH seeds are believed to form from either PoP III stars collapse (Volonteri et al. 2003) or directly from dense gas collapse (Koushiappas et al. 2004; Begelman et al. 2006) in which large quantities of gas are driven to the galaxy’s core giving rise to an accreting black hole or active galactic nucleus (AGN). Eventually, the energy outflow from the AGN

may become sufficient to halt further gas infall and truncate further star formation in the surrounding stellar spheroid, either through bright/jet mode or radio/diffuse mode feedback (e.g., Croton et al. 2006 and Somerville 2008). Although some papers also advocate AGN activity as a trigger for star formation Silk (2005) and Pipino et al. (2009). This interplay between the SMBH and its surroundings is believed to give rise to correlations between the SMBH mass and a variety of measurable properties of the host galaxy’s spheroid component.¹ After initial formation, SMBH growth is believed to progress through periodic gas accretion onto

¹ Some properties known to correlate with SMBH mass are: the spheroid luminosity L (Kormendy & Richstone 1995; Marconi & Hunt 2003); the mean velocity dispersion σ of the spheroid (Ferrarese & Merritt 2000; Gebhardt et al. 2000; Graham 2008a; Hu 2008); the spheroid mass M_{sph} (Kormendy & Richstone 1995; Marconi & Hunt 2003; Häring & Rix 2004); the galaxy light concentration C (Graham et al. 2001); the Sérsic index n of the major-axis surface brightness profile (Graham & Driver 2007). See Novak et al. (2006) for a comparative review.

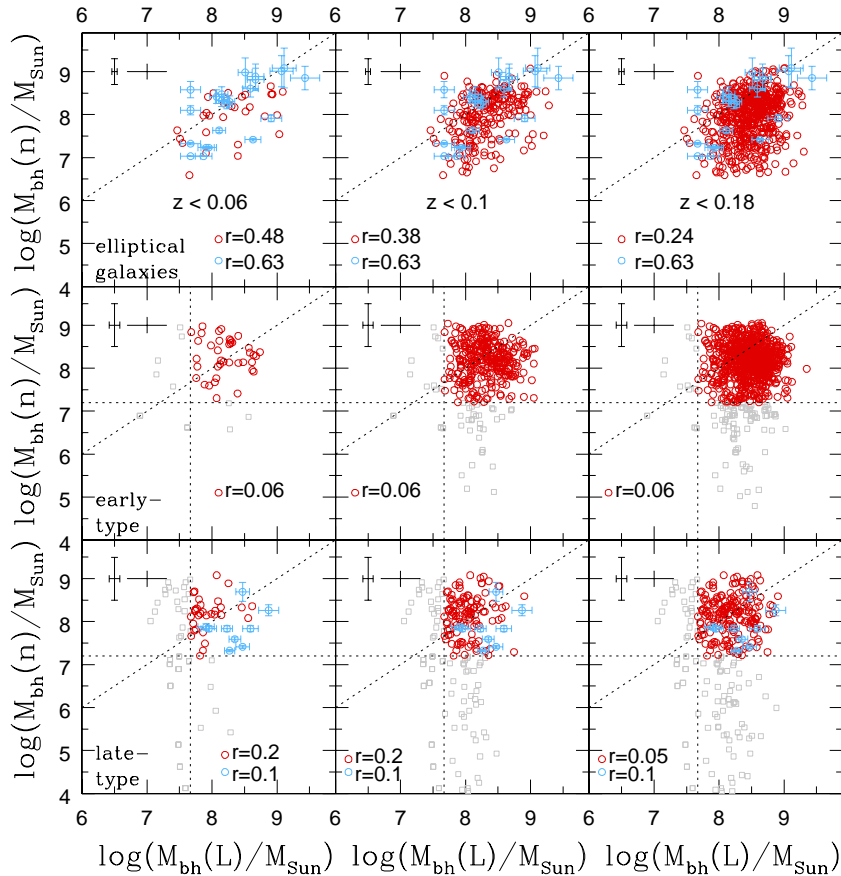


Figure 1. A comparison of SMBH masses derived from the $M_{\text{bh}}-n$ relation versus the $M_{\text{bh}}-L$ relation (left panels: $z < 0.06$, middle panels: $z < 0.1$, right panels: $z < 0.18$). The red circles are the MGC data. The blue circles denote spheroids from Caon et al. (1993). The spheroids less luminous than $M_B = -18$ mag or with Sérsic index < 2 (indicated with dashed vertical and horizontal lines, respectively) are shown as grey squares as these data are less reliable. The sloped dashed line indicates the 1-1 relation. Top panels: (left to right) 30 - 210 - 564 elliptical galaxies ($B/T = 1$), middle panel: 39 - 312 - 867 early-type disc galaxies ($1 > B/T > 0.4$), bottom panel: 34 - 109 - 312 late-type disc galaxies ($0.4 > B/T > 0.01$). The "right" error bars in each panel show the average uncertainties on the masses derived from the intrinsic scatters of the $M_{\text{bh}}-L, n$ relations and the "left" errors show those derived from the errors on the spheroid luminosities and Sérsic index (see Section 3.1). The correlation coefficient (r) has been estimated for each subsample.

the SMBH during major merger events (e.g., Granato et al. 2004; Di Matteo et al. 2005; Hopkins et al. 2008). This results in the coalescence of the SMBHs and spheroids in such a manner as to preserve these initial correlations to the present time (Robertson et al. 2006). Recent evidence does however suggest some evolution in the SMBH scaling relations and so weakening the criterion that these relations must be perfectly preserved (Shields et al. 2006; Woo et al. 2008; Shankar et al. 2009).

AGN activity peaks in the range $1 < z < 2$ (Ueda et al. 2003; Richards et al. 2006; Hopkins et al. 2007) which sets the key formation epoch for massive bulge/spheroid formation and the key merger phase of massive dark matter haloes. If the picture above is correct then the zero-redshift SMBH mass function and the cosmic AGN energy history should be closely coupled. In fact, Soltan (1982) argued that the AGN cosmic history and local SMBH mass function can be combined to determine the energy efficiency of the accretion process. Recent attempts in this direction have been made by a number of groups (e.g., Tamura et al. 2006; Hopkins et al. 2006, 2008; Shankar et al. 2009; Cao & Li 2008; Yu & Lu

2008) leading to significant conclusions. However, the credibility of these studies rests heavily on the robustness to which the local SMBH mass function has been measured and to which the cosmic AGN history is known.

Over recent years there have been a number of estimates of the SMBH mass function at zero or low redshift and a compendium of some recent results are presented in Fig. 5 of Shankar et al. (2009). Except for our previous work (Graham et al. 2007) none of these studies actually empirically measure the SMBH mass function but instead estimate it by analytically combining the measurements of the galaxy luminosity or velocity function with one of the SMBH scaling relations (as concisely outlined by Häring & Rix 2004, following the first application by Salucci et al. 1999). This inherently incorporates some assumptions of, for example, the bulge-to-disc ratio and how it varies with luminosity or how galaxy luminosity relates to galaxy velocity dispersion.

In this paper we depart from this 'analytic' approach and pursue a direct *empirical* strategy which uses the recently revised $M_{\text{bh}}-L$ relation provided by Graham (2007, his equations 6 & 19) to obtain individual SMBH masses for

each galaxy in the Millennium Galaxy Catalogue (MGC; Liske et al. 2003) which has a reliable spheroid luminosity. This complements our previous *empirical* method using the $M_{\text{bh}}-n$ relation (Graham et al. 2007) and we discuss how the two results compare.

In Section 2 we describe the data and sample selection. In Section 3 we review the latest $M_{\text{bh}}-L$ relation. In Section 4 we use this relation to calculate the SMBH mass for each galaxy and find the SMBH mass function of local galaxies, the mass density of SMBHs, the cosmological SMBH density Ω_{bh} and the baryon fraction of the Universe that is contained in central SMBHs. Finally, in Section 5 we compare our results to those previously derived from the MGC using the $M_{\text{bh}}-n$ relation and those recently summarised by Shankar et al. (2009).

A cosmological model with $\Omega_{\Lambda} = 0.7$, $\Omega_{\text{m}} = 0.3$ and $H_0 = 70 \text{ h}_{70} \text{ km s}^{-1} \text{ Mpc}^{-1}$ is adopted throughout this paper.

2 THE MILLENNIUM GALAXY CATALOGUE

The Millennium Galaxy Catalogue (MGC; Liske et al. 2003) is a medium-deep survey ($\mu_{\text{lim}} = 26 \text{ mag arcsec}^{-2}$) covering a wide region of sky (37.5 deg^2) in the B -band (4407 \AA). The survey extends 75 deg along the equator (from $9^{\text{h}} 58^{\text{m}}$ to $14^{\text{h}} 47^{\text{m}}$). The data frames were obtained using the 4-CCD mosaic Wide Field Camera on the 2.5-m Isaac Newton Telescope. Each CCD has a pixel scale of $0.333 \text{ arcsec pixel}^{-1}$. The data were taken with a median seeing $\text{FWHM} = 1.3''$.

Using the SExtractor package (Bertin & Arnouts 1996) a catalogue was derived containing over one million objects in the range $16 \leq B_{\text{MGC}} < 24 \text{ mag}$. Initially, two catalogues were defined: MGC-BRIGHT which includes all galaxies with $B < 20 \text{ mag}$ and MGC-FAINT containing the rest. For further details on the MGC imaging data and its analysis see Liske et al. (2003). MGC-BRIGHT is comprised of 10095 resolved galaxies and has 96 per cent complete redshift information (Driver et al. 2005). This sample was decomposed into bulges and discs with GIM2D using an $R^{1/n}$ Sérsic profile for bulges and an exponential profile for discs (Allen et al. 2006). The robustness of the decomposition process has been verified using duplicate observations (Allen et al. 2006) and by using extensive simulations (Cameron et al. 2009). All data and data products used in this paper are freely available.²

2.1 Sample selection

For this study we use the online catalogue `mgc-gim2d` and extract the following parameters: spheroid absolute magnitude, bulge-to-total (B/T) flux ratio, half-light radius of the bulge, redshift and weight (see Section 4). We convert the absolute magnitudes from $H_0 = 100 \text{ km s}^{-1} \text{ Mpc}^{-1}$ to $70 \text{ km s}^{-1} \text{ Mpc}^{-1}$. We additionally restrict our sample to the redshift range 0.013 to 0.18. As this sample may contain galaxies with nuclear components (e.g. star clusters) that bias the $R^{1/n}$ model, we remove all ‘spheroids’ with half-light radii

and B/T less than 0.333 arcsec (1 pixel) and 0.01, respectively (Graham et al. 2007). We note that the MGC region is overdense by 9.08 per cent (Hill et al. 2009, in prep.) and we normalise our weights accordingly.

The sample we construct here is identical to sample 3 of Graham et al. (2007) which incorporates a colour cut of $(u-r)_{\text{core}} > 2.0$. This colour cut isolates the red spheroid population and is intended to remove the predominantly blue pseudo-bulge systems. Pseudo-bulges are believed to form by a process distinct to that by which classical bulges form, and it is not yet clear whether they contain a SMBH in their centre and, if so, whether they adhere to the previously cited spheroid-SMBH relations (see Hu 2008). The colour cut adopted here follows the findings in Driver et al. (2007) of a clear colour bimodality within spheroidal systems (as also identified by Drory & Fisher 2007). After we apply the above colour cut we divide the remaining galaxies into two subsamples. The first contains 1431 ‘early-type’ galaxies ($B/T > 0.4$) and the second contains 312 ‘late-type’ galaxies ($0.01 < B/T < 0.4$).

Finally, we note that Allen et al. (2006) consider bulges with $M_{\text{B}} > -17 \text{ mag}$ to be less reliable while Graham et al. (2007) remove all galaxies fainter than $M_{\text{B}} = -18 \text{ mag}$ from their sample. In this paper we indicate the ‘unsafe’ area with a dashed vertical line at $\log(M_{\text{bh}}/M_{\odot}) = 7.67$ in all relevant figures which corresponds to $M_{\text{B}} = -18 \text{ mag}$. Data fainter than this limit should be treated with caution.

3 THE $M_{\text{BH}}-L$ RELATION

The first empirical correlation between the mass of the SMBH and the bulge luminosity was identified in the review paper by Kormendy & Richstone (1995). Following this initial study a lot of similar relations have been derived but with differing slopes for the $M_{\text{bh}}-L$ relation. As a result, for the same bulge luminosity we have a range of possible SMBH masses. This large degree of scatter that has appeared in the luminosity relation is exacerbated by the difficulties in estimating the bulge luminosity in mid-type galaxies.

Graham (2007) reviewed the relations of four studies and updated their samples with new data (including revised estimates of the distances, Hubble type classifications and SMBH masses), added new galaxies, and removed some which still have significant uncertainty in their listed values. In this paper we use the best fit from a 22 galaxy B -band sample (Graham 2007, his equation 19):

$$\log(M_{\text{bh}}/M_{\odot}) = -0.40(\pm 0.05)(M_{\text{B}} + 19.5) + 8.27(\pm 0.08), \quad (1)$$

with a total scatter of 0.34 dex in $\log M_{\text{bh}}$ and an intrinsic scatter of 0.30 dex. These 22 galaxies were derived by Graham (2007) from a parent sample of 27 galaxies from Marconi & Hunt (2003) Group I galaxies. It is important to note that this relation does not contain any corrections for internal dust attenuation. However, recently we demonstrated that dust attenuation can amount to as much as a few magnitudes in B depending on inclination (Driver et al. 2008). This poses somewhat of a dilemma as we have a choice of whether to use the final relationship presented by Graham and our original uncorrected MGC magnitudes and space densities (as used in our previous estimate of the SMBH mass function) or whether to use the dust-free $M_{\text{bh}}-L$ re-

² <http://www.eso.org/~jliske/mgc/>

Table 1. SMBH mass function data for the full, early- and late-type samples (DC = dust-corrected), as presented in Fig. 2. The uncertainties given are the 1σ values derived from the Monte Carlo simulations.

$\log_{10} M_{\text{bh}}$ [M_{\odot}]	ϕ [$10^{-4} h_{70}^3 \text{ Mpc}^{-3} \text{ dex}^{-1}$]					
	All galaxies	Early-type	Late-type	All galaxies (DC)	Early-type (DC)	Late-type (DC)
6.25	0.00 ^{+2.95} _{-0.00}	0.00 ^{+0.00} _{-0.00}	0.00 ^{+0.00} _{-0.00}	0.00 ^{+1.34} _{-0.00}	0.00 ^{+0.00} _{-0.00}	0.00 ^{+0.00} _{-0.00}
6.50	1.46 ^{+4.79} _{-1.46}	0.00 ^{+5.88} _{-0.00}	0.00 ^{+2.98} _{-0.00}	0.65 ^{+5.44} _{-0.65}	0.00 ^{+6.09} _{-0.00}	0.00 ^{+1.36} _{-0.00}
6.75	6.63 ^{+5.27} _{-5.17}	1.80 ^{+4.85} _{-1.80}	3.03 ^{+4.40} _{-3.03}	4.62 ^{+4.80} _{-3.97}	2.68 ^{+4.48} _{-2.68}	1.36 ^{+2.20} _{-1.36}
7.00	12.9 ^{+5.22} _{-5.47}	4.10 ^{+3.88} _{-2.64}	8.33 ^{+4.15} _{-4.14}	10.1 ^{+5.07} _{-4.80}	5.50 ^{+4.17} _{-3.84}	4.33 ^{+2.51} _{-2.32}
7.25	18.5 ^{+4.45} _{-4.38}	5.98 ^{+3.03} _{-2.33}	12.3 ^{+3.58} _{-3.31}	17.3 ^{+5.10} _{-5.13}	9.73 ^{+4.63} _{-4.18}	7.28 ^{+2.16} _{-2.11}
7.50	22.0 ^{+4.30} _{-3.56}	9.02 ^{+2.29} _{-2.16}	12.9 ^{+3.48} _{-2.94}	25.8 ^{+5.05} _{-4.93}	17.1 ^{+4.54} _{-4.42}	8.43 ^{+2.05} _{-1.81}
7.75	23.5 ^{+3.77} _{-3.06}	12.9 ^{+2.14} _{-1.95}	10.5 ^{+3.09} _{-2.32}	34.1 ^{+4.97} _{-4.53}	25.9 ^{+4.49} _{-4.37}	8.00 ^{+1.88} _{-1.45}
8.00	22.7 ^{+3.46} _{-2.74}	15.6 ^{+1.88} _{-1.71}	7.01 ^{+2.26} _{-1.69}	38.5 ^{+4.84} _{-4.17}	32.2 ^{+4.05} _{-3.66}	6.38 ^{+1.56} _{-1.27}
8.25	18.5 ^{+2.95} _{-2.45}	14.8 ^{+1.85} _{-1.62}	3.68 ^{+1.36} _{-1.03}	34.0 ^{+4.92} _{-4.17}	30.1 ^{+3.99} _{-3.57}	3.87 ^{+1.17} _{-0.95}
8.50	12.2 ^{+2.37} _{-2.07}	10.7 ^{+1.84} _{-1.68}	1.51 ^{+0.66} _{-0.49}	22.8 ^{+4.40} _{-4.05}	21.0 ^{+3.96} _{-3.61}	1.78 ^{+0.69} _{-0.53}
8.75	6.15 ^{+1.81} _{-1.69}	5.71 ^{+1.64} _{-1.55}	0.47 ^{+0.29} _{-0.21}	11.1 ^{+3.51} _{-3.20}	10.5 ^{+3.35} _{-3.06}	0.61 ^{+0.33} _{-0.26}
9.00	2.15 ^{+1.17} _{-0.91}	2.07 ^{+1.11} _{-0.87}	0.09 ^{+0.11} _{-0.07}	3.63 ^{+2.09} _{-1.58}	3.51 ^{+2.05} _{-1.53}	0.14 ^{+0.14} _{-0.10}
9.25	0.50 ^{+0.47} _{-0.29}	0.48 ^{+0.48} _{-0.28}	0.00 ^{+0.04} _{-0.00}	0.78 ^{+0.77} _{-0.47}	0.75 ^{+0.78} _{-0.45}	0.00 ^{+0.06} _{-0.00}
9.50	0.07 ^{+0.13} _{-0.04}	0.07 ^{+0.13} _{-0.04}	0.00 ^{+0.00} _{-0.00}	0.10 ^{+0.19} _{-0.07}	0.10 ^{+0.19} _{-0.07}	0.00 ^{+0.00} _{-0.00}

lation for elliptical galaxies (Graham 2007, his equation 6) combined with our dust corrected MGC bulge magnitudes and the correspondingly revised space densities. We choose to use and show the results of both alternatives in order to indicate the possible uncertainty introduced by dust attenuation.

3.1 Masses from $M_{\text{bh}}-L$ versus masses from $M_{\text{bh}}-n$

Graham et al. (2007) derived the SMBH mass of each galaxy in the MGC sample using the photometric quantity Sérsic index³ (n). In this paper we derive the SMBH masses using the spheroid luminosity. In Fig. 1 we directly compare the SMBH masses derived for each galaxy using the two independent methods ($M_{\text{bh}}-L$ and $M_{\text{bh}}-n$) for various subsamples defined in B/T and redshift as indicated. A correlation between the two BH mass estimates is not seen and therefore requires explaining. For each subsample we measure the linear correlation coefficient r and only the low- z elliptical systems show evidence for a correlation. For the bulges of disc galaxies, no correlation is detected.

However, we find that the lack of correlation can be well explained when one considers the errors from both the measurements (on L and n), the intrinsic scatters of the $M_{\text{bh}}-L, n$ relations, and the limited mass range probed here (see error indicators on Fig.1). In more detail, equation (1) above implies that the typical bulge luminosity error of ± 0.1 mag (see fig. 15 of Allen et al. 2006) corresponds to a mass error of ± 0.04 dex. The internal scatter of the $M_{\text{bh}}-L$, however, is ± 0.30 dex. The Sérsic index value has a typical measurement error of $\pm 20\%$ for the elliptical sample and $\pm 35\%$ for the early & late-type sample. While the internal scatter of the $M_{\text{bh}}-n$ is ± 0.18 dex (Graham et al. 2007). Hence the scatter in Fig. 1 is simply representative of the combination of two measurement errors and two intrinsic scatters (with the measurement error dominating for the $M_{\text{bh}}-n$ estimates

and the intrinsic scatter dominating for the $M_{\text{bh}}-L$ estimate) coupled with the relatively narrow range of parameter space probed.

To illustrate this conclusion we have used the same $M_{\text{bh}}-L, n$ relations as above to calculate the SMBH masses for a sample of nearby, low-inclination systems within the Virgo and Fornax clusters (Caon et al. 1993), and for which the measurement errors are, by comparison, negligible. Over the full range of parameter space explored, in this study, these data are known to give relatively tight correlations. However when overplotted (blue points on Fig. 1) for the narrow range of parameter space we probe here, they give similarly low correlation coefficients as the MGC data. This strongly suggests that the lack of correlation is mainly due to the limited range of parameter space covered by the MGC data. The lack of correlation is consistent with the adopted errors (and which are propagated throughout the analysis). The caveat is that the analysis remains susceptible to any unknown systematic errors (e.g., bar-bulge contamination) however the overlap between the MGC data and local data suggests these systematic errors cannot be a dominant factor. Finally we note that the dominant error in using the $M_{\text{bh}}-L$ relation comes from the inherent intrinsic scatter in the $M_{\text{bh}}-L$ relation rather than the MGC measurement error. Conversely the reverse is true in our previous study based on the $M_{\text{bh}}-n$ relation.

4 THE MGC SMBH MASS FUNCTION VIA $M_{\text{BH}}-L$

We have derived individual black hole masses for each spheroid using equation (1). These estimates have three sources of error. The first is the uncertainty on the parameters defining equation (1). This is a systematic error. The second source of error is the uncertainty in our spheroid magnitude measurements. Finally, as noted in the previous section, the $M_{\text{bh}}-L$ relation has significant internal scatter. We consider the latter two as random errors. (Note that the alignment of the calibration sample with the MGC sample on Fig. 1 implies that there is no obvious systematic error

³ For more information on the Sérsic index including a comprehensive review see Graham & Driver (2005).

Table 2. Results of a three-parameter Schechter function fit to the SMBH mass function, both for dust corrected (DC) and uncorrected samples. The uncertainties on the parameters were derived from Monte Carlo simulations (see text for details).

Sample	No. of spheroids	$\log \phi_*$ [$h_{70}^3 \text{ Mpc}^{-3} \text{ dex}^{-1}$]	$\log(M_*/M_\odot)$	α
All galaxies (B/T > 0.01) (DC)	1743	-3.15 ± 0.05	8.71 ± 0.08	-1.20 ± 0.10
All galaxies (B/T > 0.01)	1743	-2.92 ± 0.05	8.71 ± 0.06	-1.07 ± 0.05
Early-type (B/T > 0.4) (DC)	1431	-3.10 ± 0.05	8.64 ± 0.03	-0.90 ± 0.06
Early-type (B/T > 0.4)	1431	-2.90 ± 0.04	8.71 ± 0.03	-1.16 ± 0.10
Late-type (0.01 < B/T < 0.4) (DC)	312	-3.70 ± 0.02	8.46 ± 0.03	-1.44 ± 0.11
Late-type (0.01 < B/T < 0.4)	312	-3.66 ± 0.02	8.49 ± 0.08	-1.28 ± 0.01

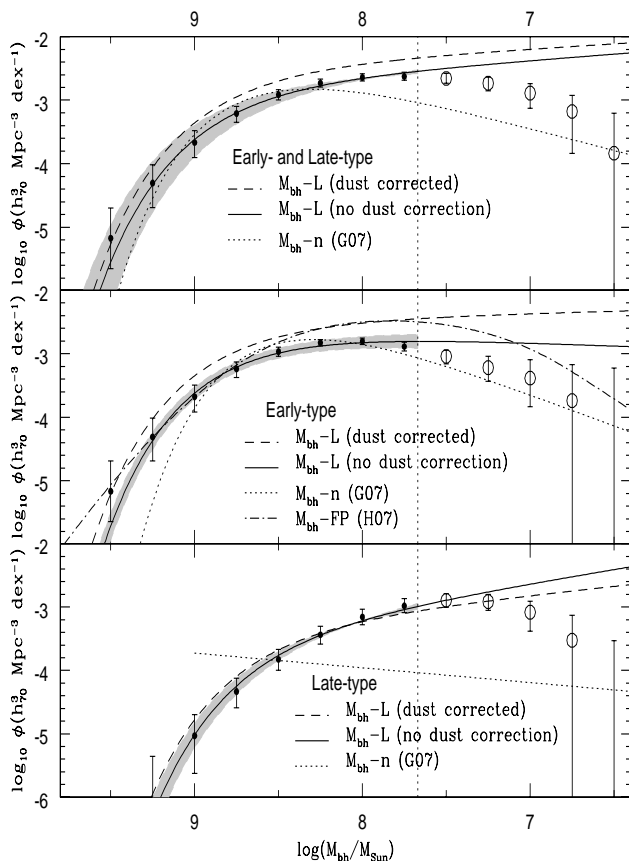


Figure 2. The data points in the top panel show the SMBH mass function of the full MGC sample. The error bars were derived from Monte Carlo simulations (see text for details). The solid line and grey shaded region represent the best fit Schechter function and its uncertainty. The dashed line shows the same for dust corrected magnitudes and weights, while the dotted line shows the result of Graham et al. (2007) using the $M_{\text{bh}}-n$ relation (corrected for the 9.08 per cent overdensity of the MGC). The middle and bottom panels show the same for our early- (B/T > 0.4) and late-type (0.01 < B/T < 0.4) samples. The dashed vertical line at $\log(M_{\text{bh}}/M_\odot) = 7.67$ (corresponding to $M_B = -18$ mag) indicates our reliability limit and we show all data beyond this limit with big open circles. The fits use only the reliable data above this limit. All data points are listed in Table 1. The additional curve in the middle panels is from Hopkins et al. (2007) (H07).

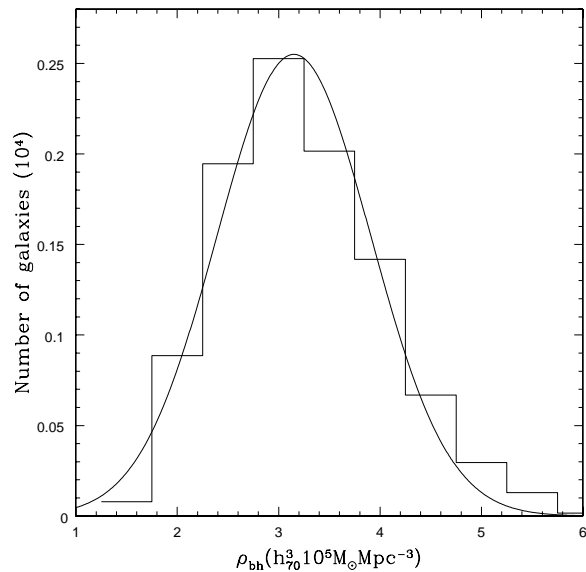


Figure 3. A histogram of the 10001 values of mass density for early-type (B/T > 0.4) galaxies from the Monte Carlo simulations. The distribution is reasonably reproduced by a Gaussian (solid line).

in our flux measurements.) To model these errors appropriately we run a series of 10001 Monte Carlo simulations. For each simulation we randomly modify the coefficients of equation (1) assuming Gaussian error distributions. We then perturb each spheroid flux by a random amount as is appropriate given the spheroid's individual magnitude error, and calculate a new set of SMBH masses from the perturbed fluxes using the perturbed version of equation (1). Finally, we randomly modify each of the SMBH masses according to the internal scatter of the $M_{\text{bh}}-L$ relation, again assuming a Gaussian distribution. Given these 10001 Monte Carlo datasets we estimate the value and 1σ error of any given quantity of interest by calculating that quantity for each of the datasets and determining the median and 68 percentile range of the resulting distribution, respectively. This procedure is similar to that followed by Graham et al. (2007).

We now wish to volume-correct our sample and to compute the SMBH mass function. To this end we employ the space-density weights derived by Driver et al. (2007): the weight of a spheroid of luminosity L is simply given by the value of the luminosity function of the appropriate spheroid type, $\phi(L)$, divided by the observed number of spheroids in

the interval $[L, L + dL]$. The value of the SMBH mass function at mass M_{bh} is then calculated as the sum of the weights of all spheroids within the interval $[M_{\text{bh}}, M_{\text{bh}} + dM_{\text{bh}}]$:

$$\phi(M_{\text{bh}}) = \sum_{[M, M+dM]} W(L), \text{ where } W(L) = \phi(L)/N(L). \quad (2)$$

In Fig. 2 we show the SMBH mass function and its errors as determined from the Monte Carlo process described above and using equation 2 for our full, early- and late-types subsamples (top to bottom). All data are listed in Table 1. In each panel of Fig. 2 the solid line represents the best fit of a three-parameter (M_*, ϕ_*, α) Schechter-like function over the mass range $10^{7.75} < M_{\text{bh}}/M_{\odot} < 10^{10}$:

$$\phi(M_{\text{bh}}) = \phi_* \left(\frac{M_{\text{bh}}}{M_*} \right)^{\alpha+1} \exp \left[1 - \left(\frac{M_{\text{bh}}}{M_*} \right) \right]. \quad (3)$$

The best fitting parameters are given in Table 2.

Finally, we integrate our Schechter-like estimation of the SMBH mass function over the mass range probed by our data to calculate the SMBH mass density, given by the expression:

$$\begin{aligned} \rho_{\text{bh}} &= \int_{\log(M_{\text{bh}}/M_{\odot})=6}^{\log(M_{\text{bh}}/M_{\odot})=10} \phi(M_{\text{bh}}) M_{\text{bh}} d \log M_{\text{bh}} \\ &= \frac{\phi_* M_* e^1}{\ln(10)} \left[\gamma \left(a + 2, \frac{10^{10} M_{\odot}}{M_*} \right) - \gamma \left(a + 2, \frac{10^6 M_{\odot}}{M_*} \right) \right] \end{aligned} \quad (4)$$

As an example of the Monte Carlo process, Fig. 3 shows the distribution of the 10001 SMBH density values. This is reasonably described by a Gaussian function. The final SMBH density is defined as the median of this distribution with the 1σ error given by 68 percentile range. The resulting mass densities of SMBHs with masses between $10^6 < M_{\text{bh}}/M_{\odot} < 10^{10}$ for the full, early- and late-type samples are given in Table 3. The last column of Table 3 also lists the corresponding cosmological density parameters $\Omega_{\text{bh}} = \rho_{\text{bh}}/\rho_{\text{crit}}$.

Integrating the mass function over *all* masses we derive slightly larger values for the densities: 5.06 (8.5), 3.8 (6.6) and $0.96 (0.92) \times 10^5 h_{70}^3 M_{\odot} \text{Mpc}^{-3}$ for the full, early- and late-type samples, respectively, where the numbers in parentheses refer to the dust-corrected values. These densities are consistent with the values reported by Graham et al. (2007).

As discussed in the introduction and also in Shankar et al. (2004) if one assumes that SMBHs form via the accretion of baryons alone and using the cosmological SMBH mass density $\Omega_{\text{bh, total}} = (3.7 \pm 0.7) \times 10^{-6} h_{70}$ we can estimate the SMBH baryon fraction. Given that $4.5 h_{70}^{-2}$ per cent of the critical density is in the form of baryons (Tegmark et al. 2006) we find that $(0.008 \pm 0.002) h_{70}^3$ per cent of the Universe's baryons are currently locked up in SMBHs at the centres of galaxies. For comparison, the value that Graham et al. (2007) found was $(0.007 \pm 0.003) h_{70}^3$ per cent.

5 DISCUSSION AND COMPARISONS TO EARLIER WORKS

Fig. 4 shows a compendium of recent estimates of the zero redshift SMBH mass function in the left panel, while the right hand panel shows the differential contribution to the

mass density. The shaded (light grey) region representing the MGC results show the spread in the means from our three estimates as tabulated in Table 2 and in Table 1 of Graham et al. (2007). Within this compendium of data only the MGC results are based on actual measurements of bulge properties. The non-MGC curves/shading all rely on coupling an empirical SMBH mass-relation with a galaxy luminosity or velocity function under some assumption as to the fraction of ellipticals and how the mean bulge-to-total ratio varies with luminosity. Typically a constant fraction for both values is adopted independent of luminosity which is contrary to what has been seen in the MGC and in other morphological studies. In reality the fraction of ellipticals and the mean B/T ratio should increase with stellar mass. Incorporating this would have the effect of tilting the mass functions derived in this ‘analytical’ way, and this is the most likely explanation for the discrepancy between some of the results shown in Fig. 4 and those from the MGC (see Appendix A for details). This echoes the recent study of nearby active systems by Greene & Ho (2007) who also find a bounded BH mass function based on an empirical study of the broad-line regions of 9000 QSOs, albeit shifted to lower black hole masses (see Fig. 4, left).

However, it is also fair to note that while the MGC results give a consistent SMBH mass density and generally agree at the high mass end they show a broader discrepancy at lower SMBH masses. Most likely this can be traced back to the bulge-disc decompositions which are no doubt imperfect, particularly for low-B/T, low-luminosity and/or low- n systems (i.e., those systems likely to contain lower mass SMBHs). Repeatability tests (Allen et al. 2006) and extensive simulations (Cameron et al. 2009) based on MGC data both show that while disc parameters are recovered extremely reliably the bulge parameters are susceptible to gross error. However, no obvious bias via the simulations has yet been seen, but rather a larger than desirable general scatter and in this manner the correct answer with appropriate errors should indeed emerge through the Monte Carlo simulation process. Note that the modelling of the SMBH mass function includes extensive Monte Carlo simulations of the structural errors along with a Malmquist Bias correction.

Within the MGC results the dominant source of random error comes from the uncertainty in the $M_{\text{bh}}-n$ and $M_{\text{bh}}-L$ relations and the associated intrinsic scatter. This is limited mainly by the sample size of the relevant calibration datasets. In terms of systematic error this most likely arises from an, as yet unknown, bias in the bulge-disc decompositions. While simulations show that systematic biases are low we do see a discrepancy between the two approaches which at this stage provides the best and only indication of the scale of any systematic. Simulations suggest that our bulge luminosity measurements are more robust than our Sérsic index measurements (reflected by the lower final errors in the SMBH mass function) and so we therefore consider the new MGC measurements based on the updated $M_{\text{bh}}-L$ relation of Graham (2007), to be superior to our previous estimate and to the other ‘analytical’ estimates (given the inherent, sometimes hidden assumptions in the analytic approach). We therefore advocate the data presented in this paper as the current best estimate of the zero redshift SMBH mass function.

Table 3. SMBH mass densities integrated over the mass range 10^6 – 10^{10} for the full, early- and late-type samples as derived from the $M_{\text{bh}}-L$ (dust corrected [DC] and uncorrected) and $M_{\text{bh}}-n$ relations (Graham et al. 2007). The differences in the numbers of spheroids are due to different absolute magnitude cuts employed. α is the error due to the uncertainties on the parameters defining equation (1) and β is from the uncertainty on the bulge magnitudes. γ is derived from the MGC global cosmic variance of 6 per cent for the effective 30.8 deg^2 region with $0.013 < z < 0.18$. Finally, δ is the error due to the intrinsic scatters of the $M_{\text{bh}}-L$ (0.30 dex) and $M_{\text{bh}}-n$ relations (0.18 dex). All densities have been corrected for the overdensity of the MGC region (9.08 per cent).

Method	No. of spheroids	$\rho_{\text{bh}} \pm \alpha \pm \beta \pm \gamma \pm \delta$ [$10^5 h_{70}^3 M_{\odot} \text{ Mpc}^{-3}$]					Ω_{bh} [$10^{-6} h_{70}$]
Full sample (B/T > 0.01):							
$M_{\text{bh}}-L$	1743	4.9 ± 0.7	± 0.5	± 0.3	± 0.1	3.7 ± 0.7	
$M_{\text{bh}}-L_{\text{DC}}$	1743	8.0 ± 1.3	± 0.4	± 0.5	± 0.3	6.2 ± 1.1	
$M_{\text{bh}}-n$	1543	4.0 ± 1.5	± 0.06	± 0.2	± 0.04	2.9 ± 1.1	
Early-type (B/T > 0.4):							
$M_{\text{bh}}-L$	1431	3.8 ± 0.6	± 0.4	± 0.2	± 0.1	2.5 ± 0.3	
$M_{\text{bh}}-L_{\text{DC}}$	1431	6.5 ± 1.2	± 0.3	± 0.4	± 0.3	4.8 ± 0.6	
$M_{\text{bh}}-n$	1352	3.1 ± 1.04	± 0.05	± 0.2	± 0.03	2.3 ± 0.8	
Late-type (0.01 < B/T < 0.4):							
$M_{\text{bh}}-L$	312	0.96 ± 0.2	± 0.05	± 0.06	± 0.07	0.7 ± 0.2	
$M_{\text{bh}}-L_{\text{DC}}$	312	0.92 ± 0.1	± 0.04	± 0.05	± 0.05	0.7 ± 0.1	
$M_{\text{bh}}-n$	191	0.86 ± 0.49	± 0.03	± 0.05	± 0.02	0.6 ± 0.4	

SMBH mass functions derived from the $M - \sigma$ relation also show an increase in density towards low black hole masses. However velocity dispersions for the lower mass systems are generally estimated rather than measured with a number of hidden implicit assumptions required (e.g., Aller & Richstone 2002). The most recent studies (Lauer et al. 2007; Tundo et al. 2007) use the velocity dispersion function from Sheth et al. 2003, however this function estimates the black hole masses from the systemic circular velocity which could lead to an overestimation of SMBH masses and a steeper faint-end.

6 CONCLUSIONS

We have used a sample of 1743 galaxies extracted from the Millennium Galaxy Catalogue to estimate the SMBH masses from the $M_{\text{bh}}-L$ relation (using Graham 2007, his equation 19) to construct the SMBH mass function at redshift zero. Our results agree well with our previous study, however, in comparison to other published data the MGC data consistently show a steep drop-off or decline in the space-density of SMBHs towards lower masses. Although this lies below what we consider to be our reliable limits ($< 10^7 M_{\odot}$) it most likely arises from our more direct empirical approach. Essentially, the SMBH mass function declines because the spheroid luminosity function declines (Driver et al. 2007).

Within our reliability limits the contribution of the SMBH mass function to the total cosmic SMBH density budget is sharply peaked. Integrating over the best fit mass function we obtain a total SMBH mass density of $\rho_{\text{bh}} = (4.90 \pm 0.7) \times 10^5 h_{70}^3 M_{\odot} \text{ Mpc}^{-3}$ and a cosmological SMBH density of $\Omega_{\text{bh}} = (3.7 \pm 0.7) \times 10^{-6} h_{70}$. This implies that $(0.008 \pm 0.002) h_{70}^3$ per cent of the Universe’s baryons are contained in SMBHs, in excellent agreement with the results from Graham et al. (2007).

In this, and our previous, paper we have measured the SMBH mass function via three methods. Once using the $M_{\text{bh}}-n$ relation (Graham et al. 2007) and twice using the $M_{\text{bh}}-L$ relation (this paper; once ignoring dust attenuation

and once correcting for dust attenuation). From a comparison of the three SMBH mass functions we find that the discrepancy in any one bin of the SMBH mass function (probably the most realistic quantitative insight into the hidden systematic errors) lies at the 30 per cent level. This constitutes the current limit which can be achieved from the MGC dataset. A significant improvement can be made in three ways. Firstly, by increasing the sample size, secondly by obtaining more robust measurements, and thirdly by improving the accuracy in which the $M_{\text{bh}}-L, n$ relations are known. One obvious direction in the latter case is to re-derive the $M_{\text{bh}}-L, n$ relations in the NIR to overcome the severe effects of dust attenuation (see Driver et al. 2007). At the present time no suitable catalogue exists. Over the coming years we are embarking on a programme to recalibrate the $M_{\text{bh}}-L, n$ relations at near-IR wavelengths (where we expect the intrinsic scatter to be significantly reduced), as well as construct a $\sim 100\times$ larger NIR-selected galaxy sample ($\approx 240\text{k}$ galaxies via the ongoing Galaxy And Mass Assembly survey; Driver 2008). With these two improvements we should be able to significantly reduce the errors inherent in this work as well as probe a significantly broader black hole mass range.

ACKNOWLEDGMENTS

The Millennium Galaxy Catalogue consists of imaging data from the Isaac Newton Telescope and spectroscopic data from the Anglo-Australian Telescope, the ANU 2.3-m, the ESO New Technology Telescope, The Telescope Nazionale Galileo, and the Gemini Telescope. The survey has been supported through grants from the Particle Physics and Astronomy Research Council (UK) and the Australian Research Council (AUS). We thank the referee for helpful suggestions that improve this paper. The data and data products are publicly available from <http://www.eso.org/~jliske/mgc/> or on request from J. Liske or S.P. Driver.

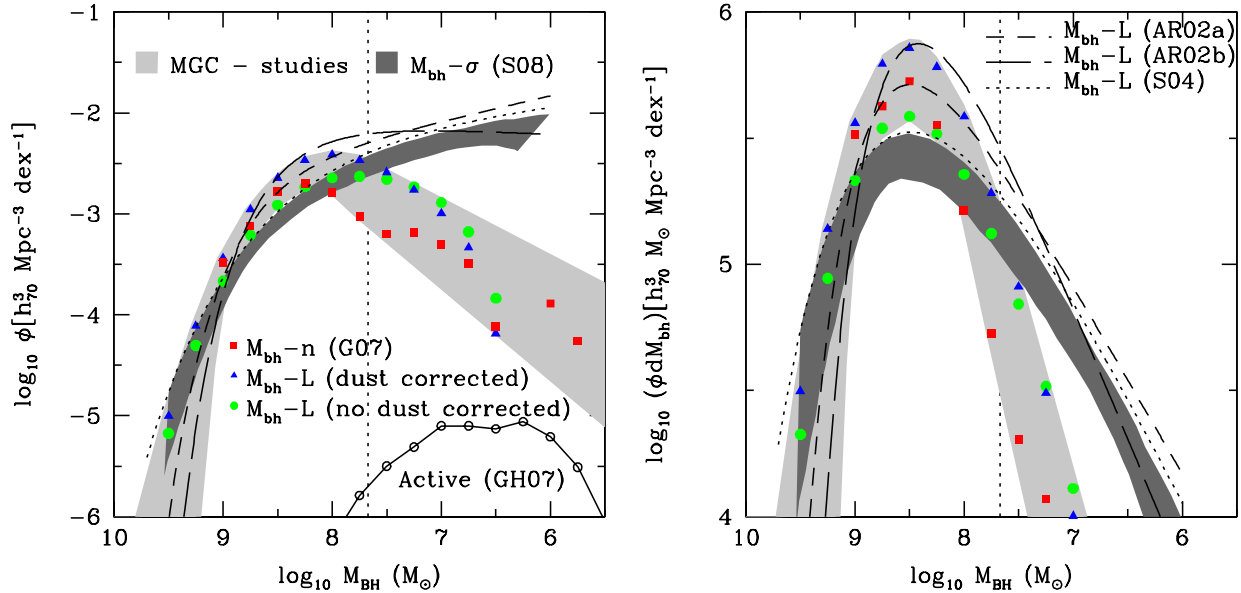


Figure 4. Left panel: a compendium of zero redshift SMBH mass functions corrected for the hidden Hubble dependency. The curves are from Shankar et al. (2004) (S04); Aller & Richstone (2002) (AR02a, AR02b); Greene & Ho (2007) (GH07) and Shankar et al. (2009) (S08, $z=0$ curve). The light grey shaded region represents the MGC results from our three estimates. The data points show the SMBH mass function for all the MGC subsamples (red squares: Graham et al. (2007); blue triangles: this study, dust corrected; green circles: this study, no dust corrected). Right panel: equivalent plot showing the contribution by SMBH mass to the cosmic SMBH mass density.

REFERENCES

- Allen P. D., Driver S. P., Graham A. W., et al., 2006, *MNRAS*, 371, 2
- Aller M. C., Richstone D., 2002, *AJ*, 124, 3035
- Balcells M., Graham A. W., Peletier R. F., 2007, *ApJ*, 665, 1104
- Begelman M. C., Volonteri M., Rees M. J., 2006, *MNRAS*, 370, 289
- Bertin E., Arnouts S., 1996, *A&AS*, 117, 393
- Cameron E., Driver S. P., Graham A. W., Liske J., 2009, *ApJ*, 699, 105
- Cao X., Li F., 2008, *MNRAS*, 390, 561
- Caon N., Capaccioli M., D’Onofrio M., 1993, *MNRAS*, 265, 1013
- Croton D. J., Springel V., White S. D. M., De Lucia G., Frenk C. S., Gao L., Jenkins A., Kauffmann G., Navarro J. F., Yoshida N., 2006, *MNRAS*, 365, 11
- Di Matteo T., Springel V., Hernquist L., 2005, *Nat*, 433, 604
- Driver S. P., Allen P. D., Graham A. W., et al., 2006, *MNRAS*, 368, 414
- Driver S. P., Allen P. D., Liske J., Graham A. W., 2007, *ApJL*, 657, L85
- Driver S. P., Liske J., Cross N. J. G., et al., 2005, *MNRAS*, 360, 81
- Driver S. P., Popescu C. C., Tuffs R. J., et al., 2007, *MNRAS*, 379, 1022
- Driver S. P., Popescu C. C., Tuffs R. J., et al., 2008, *ApJ*, 678, L101
- Drory N., Fisher D. B., 2007, *ApJ*, 664, 640
- Ferrarese L., Côté P., Dalla Bontà E., Peng E. W., Merritt D., Jordán A., Blakeslee J. P., Hasegan M., Mei S., Piatek S., Tonry J. L., West M. J., 2006, *ApJL*, 644, L21
- Ferrarese L., Merritt D., 2000, *ApJ*, 539, L9
- Gallo E., Treu T., Jacob J., Woo J.-H., Marshall P. J., Antonucci R., 2008, *ApJ*, 680, 154
- Gebhardt K., Bender R., Bower G., et al., 2000, *AJ*, 539, L13
- Graham A., Erwin P., Caon N., Trujillo I., 2001, *AJ*, 563, L11
- Graham A. W., 2007, *MNRAS*, 379, 711
- Graham A. W., 2008a, *ApJ*, 680, 143
- Graham A. W., 2008b, *PASA*, 25, 167
- Graham A. W., Driver S. P., 2005, *Publications of the Astronomical Society of Australia*, 22, 118
- Graham A. W., Driver S. P., 2007, *ApJ*, 655, 77
- Graham A. W., Driver S. P., Allen P. D., Liske J., 2007, *MNRAS*, 378, 198

Graham A. W., Guzmán R., 2003, *AJ*, 125, 2936
 Granato G. L., De Zotti G., Silva L., Bressan A., Danese L., 2004, *ApJ*, 600, 580
 Greene J. E., Ho L. C., 2007, *ApJ*, 667, 131
 Häring N., Rix H. W., 2004, *ApJ*, 604, L89
 Hopkins P. F., Hernquist L., Cox T. J., Di Matteo T., Robertson B., Springel V., 2006, *ApJs*, 163, 1
 Hopkins P. F., Hernquist L., Cox T. J., Kereš D., 2008, *ApJs*, 175, 356
 Hopkins P. F., Hernquist L., Cox T. J., Robertson B., Krause E., 2007, *ApJ*, 669, 45
 Hopkins P. F., Richards G. T., Hernquist L., 2007, *ApJ*, 654, 731
 Hu J., 2008, *MNRAS*, 386, 2242
 Kormendy J., Richstone D., 1995, *ARA&A*, 33, 581
 Koushiappas S. M., Bullock J. S., Dekel A., 2004, *MNRAS*, 354, 292
 Lauer T. R., Tremaine S., Richstone D., Faber S. M., 2007, *ApJ*, 670, 249
 Liske J., Lemon D. J., Driver S. P., et al., 2003, *MNRAS*, 344, 307
 Magorrian J., Tremaine S., Richstone D., et al., 1998, *AJ*, 115, 2285
 Marconi A., Hunt L. K., 2003, *AJ*, 589, L21
 Novak G. S., Faber S. M., Dekel A., 2006, *ApJ*, 637, 96
 Pipino A., Silk J., Matteucci F., 2009, *MNRAS*, 392, 457
 Richards G. T., Strauss M. A., Fan X., Hall P. B., Jester S., Schneider D. P., Vanden Berk D. E., et al., 2006, *AJ*, 131, 2766
 Robertson B., Cox T. J., Hernquist L., Franx M., Hopkins P. F., Martini P., Springel V., 2006, *ApJ*, 641, 21
 Salucci P., Szuszkiewicz E., et al., 1999, *MNRAS*, 307, 637
 Satyapal S., Vega D., Dudik R. P., Abel N. P., Heckman T., 2008, *ApJ*, 677, 926
 Shankar F., Bernardi M., Haiman Z., 2009, *ApJ*, 694, 867
 Shankar F., Salucci P., Granato G. L., De Zotti G., Danese L., 2004, *MNRAS*, 354, 1020
 Shankar F., Weinberg D. H., Miralda-Escudé J., 2009, *ApJ*, 690, 20
 Sheth R. K., Bernardi M., Schechter P. L., Burles S., Eisenstein D. J., et al., 2003, *ApJ*, 594, 225
 Shields G. A., Menezes K. L., Massart C. A., Vanden Bout P., 2006, *ApJ*, 641, 683
 Silk J., 2005, *MNRAS*, 364, 1337
 Soltan A., 1982, *MNRAS*, 200, 115
 Somerville R. S., 2008, arXiv:0808.1254
 Tamura N., Ohta K., Ueda Y., 2006, *MNRAS*, 365, 134
 Tegmark M., Eisenstein D. J., Strauss M. A., Weinberg D. H., Blanton M. R., et al., 2006, *Phys.Rev.D.*, 74
 Tundo E., Bernardi M., Hyde J. B., Sheth R. K., Pizzella A., 2007, *ApJ*, 663, 53
 Ueda Y., Akiyama M., Ohta K., Miyaji T., 2003, *ApJ*, 598, 886
 Volonteri M., Haardt F., Madau P., 2003, *ApJ*, 582, 559
 Woo J.-H., Treu T., Malkan M. A., Blandford R. D., 2008, *ApJ*, 681, 925
 Yu Q., Lu Y., 2008, *ApJ*, 689, 732

APPENDIX A: PREDICTING THE SMBH MASS FUNCTION DIRECTLY FROM THE GALAXY LUMINOSITY FUNCTION

In this paper we have derived the nearby SMBH mass function through direct estimates of SMBH masses for 1743 individual galaxies selected from the Millennium Galaxy Catalogue (MGC; see Sample 3 definition described in Graham et al. 2007). Our resulting SMBH mass function determined using the $M_{\text{bh}}-L$ relation is consistent with our earlier estimate based on the $M_{\text{bh}}-n$ relation and those derived analytically as shown in Fig. 4. However, below our limit of bulge reliability (i.e., $M_B > -18$ mag) we note a sharp decline in our mass function not mirrored in the analytical estimates. In Section 5 we claim this is due to inherent assumptions in the analytical process related to the accuracy to which type fractions are known and the adoption of a constant bulge-to-total luminosity ratio. To understand why this is so we firstly describe the analytical method, we then explore some of the implicit assumptions, and finally derive a set of analytical SMBH mass functions to illustrate the basis of these claims. We note that to fully explore this issue it is necessary to revert to the full MGC sample for which some fraction of our bulge measurements will be unreliable (see Cameron et al. 2009 for a detailed discussion of these issues). We therefore make a strong caveat that the values and results reported in this appendix are to qualitatively illustrate some of the subtleties in estimating the SMBH mass function analytically only and are not sufficiently robust to produce definitive SMBH mass function estimates at this time.

A1 Estimating SMBH mass functions analytically

Apart from our empirical studies, all estimates of the SMBH mass function combine a global galaxy luminosity function with estimates of population ratios and bulge-to-total luminosity ratios. This situation arises because the Millennium Galaxy Catalogue is the only study, to date, to actually separate the bulge and disc components for a sufficiently large sample (Allen et al. 2006). In the analytical approach using, for example, the $M_{\text{bh}}-L$ method, a galaxy luminosity function is adopted (or a set of Hubble type specific luminosity functions) and the space-density of bulges is then estimated by adopting a constant bulge-to-total flux ratio (or a set of bulge-to-disc flux ratios for each Hubble type). These estimated bulge luminosity functions can then be convolved with the $M_{\text{bh}}-L$ expression to produce an analytic SMBH mass function. There are three main issues with this technique: (i) Hubble population fractions are not well constrained and depend on luminosity (while type dependent luminosity functions will accommodate for this, estimates based on the global luminosity function typically do not). (ii) Bulge-to-total flux ratios are believed to vary with luminosity (typically all systems fainter than $M_B = -17$ mag are single component only) and this has not yet been adequately quantified. (iii) A final more subtle issue is the distinction between the type of bulge, simple Hubble classification does not distinguish between red bulges (classic) and blue bulge (possible pseudo-bulges or contaminant bars). Our assertion in this paper has been to only predict SMBH masses for red-

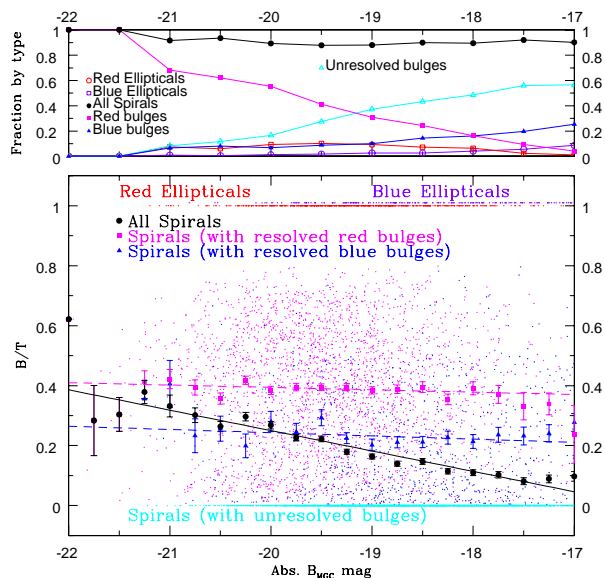


Figure A1. (*main panel*) The distribution of B/T versus absolute magnitude for various galaxy sub-populations (as indicated). Overlaid are the mean trends and errors on the mean for the red-bulge (solid squares), blue-bulge (solid triangles), and combined spiral population (solid circles). (*upper*) The relative fraction of various galaxy sub-populations colour coded as in the main panel.

bulge systems as it is unclear at this time whether blue-bulge systems also harbor SMBHs.

A2 MGC B/T dependency with luminosity

Returning to the full publicly available MGC catalogue we can directly determine the dependency of bulge type and bulge-to-total ratio as a function of luminosity. First we restrict the sample (to minimise the contamination by spurious bulges) to the redshift range $0.013 < z < 0.18$ leaving 7044 galaxies from a parent sample of 10095. We now construct the following sub-populations (following the arguments laid down in earlier MGC papers):

- (1) Red bulge-only (elliptical) systems ($B/T = 1$, $(u-r)_c > 2$), 579
- (2) Blue bulge-only (elliptical) systems ($B/T = 1$, $(u-r)_c < 2$), 235
- (3) Red bulge systems ($0 < B/T < 1$, $(u-r)_c > 2$), 2487
- (4) Blue bulge systems ($0 < B/T < 1$, $(u-r)_c < 2$), 964
- (5) Bulge-less or unresolved bulge systems ($B/T = 0$), 2779

We plot these populations on the main panel of Fig. A1. Solid points show the mean B/T for the red and blue bulge systems as well as that for the combined spiral sample (red bulge, blue bulge and bulge-less systems) versus absolute magnitude. We see that the bulge-to-total fraction of the individual red and blue bulge populations are distinct but relatively constant. In contrast the overall mean spiral B/T shows a linear decrease (reasonably well described by the relation $B/T = -1.09 - 0.067M_B$).

In the top panel of Fig. A1 we show how the fraction of each population varies. At bright luminosities the sample is dominated by red-bulge systems which steadily declines, in

turn we see a corresponding rise in blue-bulge and bulge-less systems. The trends seen are quite distinct showing minimal scatter in the measurement of the means, this suggests that while errors in some of our bulge measurements are no doubt present they are unlikely to be dominating.

A3 Derivation of the SMBH mass function through scaling relations

We can now adopt a global galaxy luminosity function (e.g., that derived in B for the MGC itself in Driver et al. 2006) and combine this with the scaling relations seen in A1 under various assumptions as follows:

Method 1 — Adopt a constant B/T and a constant spiral fraction (standard practice).

Method 2 — Adopt a varying B/T and a constant spiral fraction.

Method 3 — Adopt a constant B/T and the red bulge fraction (similar to our Sample 3).

Method 4 — Adopt a constant B/T and the red and blue bulge fraction.

Fig. A2 (upper panel) shows the global MGC luminosity function (red/solid) and the implied bulge luminosity functions based on these four methods outlined above. Fig. A2 (lower panel) shows the implied SMBH mass function. We can see that the faint end of the SMBH mass function depends critically on these relations and our assumptions. In particular the key question arises as to whether blue bulge system (potentially pseudo-bulge systems) harbor SMBHs or not and if so whether they follow the same trends as classical (red) bulges. In conclusion, and having explored both methods, we continue to advocate the empirical approach laid out in the main body of this paper, where every bulge has been measured, and the errors have been derived from Monte Carlo simulations, over the analytical approach with its hidden assumptions.

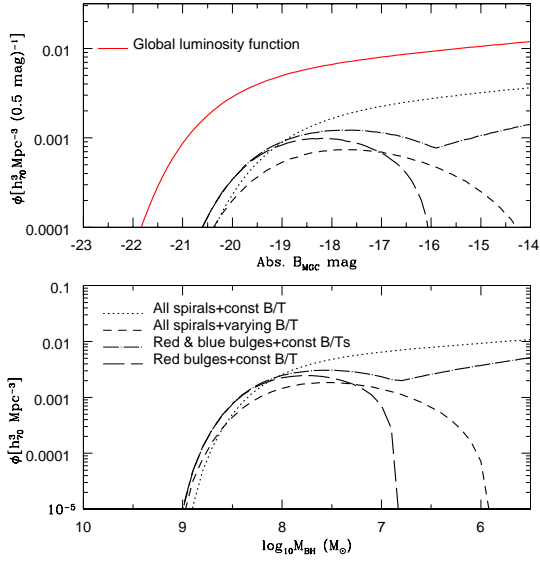


Figure A2. (*upper panel*) The global B-band galaxy luminosity function from Driver et al. (2005) and a variety of bulge luminosity functions one might derive (as described in the text). (*lower panel*) The resulting analytical SMBH mass functions depending which model LF is adopted.